Current Topics in Electrochemistry
Vol. 25, 2023

Original Article

Corrosion of copper in simulated waters during final disposal of spent nuclear fuel

Jari Aromaa*, Iryna Makarava and Mari Lundström
Aalto University, School of Chemical Engineering, P.O. Box 16200, 00075 Aalto, Espoo, Finland.

ABSTRACT

The processing of a copper canister for the final disposal of spent nuclear fuel causes oxidation of the canister surface as the spent fuel will increase its temperature. The maximum surface temperature can be close to 100 °C. The oxide film on copper may protect from corrosion or increase the corrosion rate. Corrosion was studied using weight loss tests. The baseline corrosion rate was determined by using long-term interval tests at room temperature and the effect of temperature was studied using short-term tests at temperatures up to 80 °C. The test environments were synthetic groundwater with total dissolved solids of 10070 mg/l and pH = 8 and bentonite clay pore water with total dissolved solids of 3360 mg/l and pH = 10. Both waters were tested under air and nitrogen purging. After 40 months of immersion at room temperature, the corrosion rates in groundwaters were 4-6 µm y^{-1} and in pore waters less than one µm y^{-1}. At elevated temperatures, the corrosion rates increased with increasing temperature. The highest corrosion rates at 80 °C were 60-80 µm y^{-1} in air-purged groundwater and about 30 µm y^{-1} in nitrogen-purged groundwater. In air-purged pore water, the highest corrosion rates at 80 °C were 8-9 µm y^{-1} and in nitrogen-purged waters 2-4 µm y^{-1}. In most of the tests, the air-formed oxide films protected from corrosion or did not affect corrosion. Only in the nitrogen-purged pore waters did the oxide films sometimes increase the corrosion rate. The corrosion rate increases were only a few µm y^{-1}, and this was concluded not to have a significant effect on the copper canister lifetime.

KEYWORDS: copper, corrosion, canister, spent nuclear fuel, lifetime prediction.

INTRODUCTION

Deep geological disposal is planned for nuclear waste management in most countries. The only disposal site under construction is the Finnish Onkalo, and its commission is planned for 2024. Planned projects with a selected site are in France, Russia, Sweden, and Switzerland with commission dates in the 2030s or later [1]. The Finnish plan for the final deposition of spent nuclear fuel is based on the KBS-3 concept. The acronym KBS comes from the Swedish word Kärnbränslesäkerhet (nuclear fuel safety), and the number 3 signifies the version. The acronym KBS has been used since 1976, and version 3 with the corrosion-resistant copper canister was adopted in 1983 [2]. Copper was selected as the canister material because copper is the most noble and thermodynamically stable of the common construction materials. Metallic copper is still found in nature, and this was taken as evidence that copper can withstand corrosion in natural environments [2].

In the KBS concept, the spent fuel is encapsulated in canisters that are gas-tight, corrosion-resistant, and mechanically strong. Details of the disposal system safety functions are described in [3, 4]. The spent fuel assemblies are placed in load-bearing inserts made of cast iron. These inserts are then placed into corrosion-resistant copper

*Corresponding author: jari.aromaa@aalto.fi

canisters that are sealed by friction stir welding. The canisters are placed in bedrock at a depth of about 400 to 700 meters to isolate the encapsulated spent fuel from the surface environment. In the deposition holes, the canisters are surrounded by a compacted bentonite clay buffer that prevents the flow of groundwater to the canister surface and protects canisters from rock movements. Finally, the tunnels and cavities in the bedrock used for the deposition of canisters are backfilled and closed. The long-term containment is planned so that the safety functions shall effectively prevent the release of disposed radioactive materials into the bedrock for at least hundreds of thousands of years.

After the emplacement of the canisters in the bedrock, the corrosive environment around the canister will be a combination of initial bentonite clay pore water and groundwater saturating slowly the bentonite. The nature of the near-field environment will evolve with time as the repository environment returns to its pre-excavation state as the heat dissipates, oxidants are consumed, and other redox processes start to take place [5]. When the canister cools down and the trapped atmospheric oxygen has been used up, the repository environment will become cool and anoxic. From a corrosion point of view, the conditions will be saturated and anoxic for over 99% of the canister service life [6]. The first period with warm and oxidizing conditions is considered as the most corrosive. This period will last from less than a year to some years [5]. During this period chlorides and entrapped oxygen are the major contributors to corrosion. In chloride-containing systems, cupric species can also act as oxidants, and they can be reoxidized by entrapped oxygen [7]. General corrosion rates by model estimates are from 4-6 μm y^{-1} [8] to about 10 μm y^{-1} [5]. Experiments in synthetic waters and brines have shown corrosion rates from 2 μm y^{-1} [9] to 20 μm y^{-1} [10, 11] depending on salinity, temperature, and oxidizing conditions. When the system contains bentonite clay and the environment pH is high, the measured corrosion rates have been from less than one μm y^{-1} [12-15] to 2-3 μm y^{-1} [15-17].

After loading and assembly of the canister, the spent fuel will cause an increase in the canister temperature. The canister surface temperature can reach close to 100 °C when in a radiation shield or deposition hole with unsaturated bentonite buffer [18, 19]. The time from assembly to final emplacement can be up to a few months, and most of that time the canisters are in underground storage [18, 20]. Before emplacement, the copper canister will develop an oxide layer of CuO and Cu_2O, and its thickness has been estimated as a few tens or few hundreds of nanometers [19, 21]. In pH = 9.2 borate buffer, the oxygen reduction on copper was inhibited by a $Cu/Cu_2O/CuO$ duplex layer that formed when copper was oxidized [22], and the cupric species in the layer were responsible for the inhibition [23]. In 1 M NaCl solution, a surface containing both metallic copper and Cu(I) species like $Cu(OH)_{ads}$ and Cu_2O was reported to be more catalytic to oxygen reduction than metallic copper [24]. On the other hand, a fully covering Cu_2O layer inhibited oxygen reduction [24]. Cu_2O can increase the total cathodic reaction rate by its own reduction, and this could result in slightly faster corrosion [25]. Also, in [26, 27] it is stated that both in sulfate and chloride solutions the partial reduction of existing Cu_2O can increase the oxygen reduction rate. Based on mixed potential theory an increase in cathodic oxygen reduction reaction rate will increase copper corrosion rate.

The copper canister is the most important barrier against the release of spent nuclear fuel. The general corrosion rate of copper depends on the cathodic reduction of cupric species and oxygen and copper surface passivation. The general corrosion rate can be affected by air-formed oxide films on copper. This is a detail that has not been included in canister life estimates documented for example in [6]. In this study, we have used weight loss tests in different synthetic waters and compared the corrosion rates of non-oxidized and oxidized samples to find out, if there are general trends in how the oxide films affect corrosion rate, and if the oxide films can significantly affect the lifetime of the canister.

MATERIALS AND METHODS

The corrosion rates were measured as weight loss during immersion. The immersion tests were divided into long-term tests at room temperature and short-term tests at elevated temperatures of 40 °C, 60 °C, and 80 °C. The long-term tests were

arranged as interval tests using 2-month and 10-month intervals. The first tests were started in July 2019 and the last ones finished in December 2022. Short-term tests lasted 3 to 6 weeks.

Samples were 30 mm by 30 mm cut from 1 mm thick oxygen-free copper sheet CW008A with a 3 mm hole drilled for mounting. The weight of the sample was about 8 grams, and the surface area 19.05 cm^2. Before the tests samples were degreased in ethanol and pickled in 10 wt-% citric acid at room temperature three times for five minutes and then rinsed with Millipore purified water and ethanol. The oxidized samples were put in the oven immediately after cleaning and weighing. Sets of five replicate samples were hung using thin PVDF-insulated copper wire with short plastic tubes separating the samples. After the tests, the samples were cleaned by immersion in 10 wt-% citric acid and using a soft nylon brush. In some cases, the corrosion product films were very adherent, and cleaning required hours. Too long immersion in cleaning was noticed as a risk of excessive weight loss and therefore too high calculated corrosion rate. Immersion of clean samples in citric acid caused sample weight loss rate of 3-3.5 µg min^{-1} corresponding to a corrosion rate of 90-110 µm y^{-1}. Therefore, cleaning times were kept as short as possible to get a sample without corrosion products but without an overestimated corrosion rate due to sample dissolution.

The corrosion rate was calculated from the weight loss and immersion time using equation (1), where Δm is weight change [g], A is sample area [cm^2], t is time [days], and ρ is density of copper 8.96 g cm^{-3}. Every sample set contained five replicate samples and the weight loss results are calculated as averages and error estimates as standard deviation divided by the square root of the number of samples.

$$CR\ [\mu m\ y^{-1}] = \Delta m / (A \cdot t \cdot \rho) \cdot 3650000 \quad (1)$$

The test waters were synthetic groundwater (coded GW) and bentonite clay pore water (PW). Both waters were purged with air and nitrogen to control the concentration of dissolved oxygen. The groundwater was adapted from Olkiluoto final deposition site groundwaters [28] and pore water was adapted from [29]. The water compositions are shown in Table 1.

The effects of oxide films were studied by using non-oxidized samples (coded CU) and samples oxidized in a drying oven with continuous air flow (Pol-Eko SLW 53 Smart, Pol-Eko Aparatura,

Table 1. Composition of the test waters.

Component	Ground water (GW), mg/l	Pore water (PW), mg/l
Na	3610	1000
Cl	5340	80
SO_4	582	1300
Ca	279	4
Mg	102	4
K	87.5	12
Br	42	
HCO_3	13.7	960
Sr	7.71	
Si	6.25	
B	1.38	
F	0.74	
Mn	0.168	
pH	7.9	10
TDS	10070	3360

Wodzisław Śląski, Poland). The oxidation times were 3 days at 60 °C (light oxidation, coded LI) or 7 days at 100 °C (heavy oxidation, coded HE). The light oxidation resulted in 40 nm thick layer of Cu_2O and heavy oxidation in 100 nm thick layer with mostly Cu_2O and a small amount of CuO [21].

Samples were weighed using Mettler TOLEDO XSE205 balance with 81 g range and 0.01 mg resolution. At the beginning of every weighting session, the balance was checked using a 20 g reference weight. All weightings were done 3 to 6 times.

The test vessels in long-term tests were 75-liter food-grade polyethylene vessels containing 50 liters of test water. In short-term tests, one-liter water-jacketed glass reactors were used. Water monitoring was done using Hanna Instruments HI98194 Multiparameter Meter. The parameters that were followed were pH, dissolved oxygen, total dissolved solids, and temperature. In long-term tests, the evaporated water was topped up with purified water during water monitoring or sample changing.

To estimate the effect of the oxide film on corrosion, the corrosion rates of non-oxidized and oxidized sample sets were analyzed using the Microsoft Excel Data Analysis Tool t-Test: Two-Sample Assuming Unequal Variance combined with Box-and-Whisker plots. The null hypothesis of the analysis was that the corrosion rates of oxidized and non-oxidized samples are the same.

Surface morphology and composition of corrosion products were studied using Mira2 Tescan GM (Czech Republic) scanning electron microscopy (SEM) equipped with an energy dispersive X-ray (EDS, Thermo Fisher Scientific, U.S.A.) unit. The accelerating voltage for SEM and EDS was 10 kV and 20 kV, respectively. Live time limit for EDS spectrum was 20 sec. The copper corrosion layer chemical composition and crystal structure after corrosion tests were further studied using X-ray diffraction (XRD) (Bruker D8 Advance) with Cu Kα irradiation. The 2θ range was 10–90° and the step size was 0.05 $°s^{-1}$.

RESULTS

The results include long-term weight loss tests to get baseline corrosion rates and short-term tests to study the effect of temperature. Corrosion product film analyses give indications of copper passivation.

Long-term room temperature tests

The long-term tests at room temperature lasted from July 2019 to December 2022. One 10-month interval and three 2-month interval tests were completed, Figure 1. During the tests the pH in groundwaters varied between 7.7 and 8.9, and in pore waters between 9.6 and 10.6. The concentration of dissolved oxygen was between 4.7 and 8.0 ppm in air-purged waters and between 0.3 and 4.9 ppm in nitrogen-purged waters. The purging of nitrogen was 0.5 dm^3 min^{-1} and it was not always enough to keep the dissolved oxygen at the target level less than 1 ppm. In short-term tests the concentration of dissolved oxygen in air-purged waters was 6-7 ppm and in nitrogen-purged waters less than 1 ppm. Problems with the gas purging were due to the blocking of gas distribution sinters by deposits and the unintentional closing of gas distribution lines in the building. In the groundwater tests, the total dissolved solids increased from about 12000 ppm to 15000 ppm. In pore water tests the total dissolved solids (TDS) was between 2300 ppm and 3200 ppm.

The corrosion rates measured in the long-term tests are shown in Figures 2-5 in the chronological order the sample sets were taken out from immersion. In long-term tests in groundwater with air purging the corrosion rate decreased with time, Figure 2. The decrease in corrosion rate with increasing test length is usually due to the formation of reaction product layers. This can be seen in the 2, 4, and 8-month tests in 2019 and 2020. The nearly constant corrosion rates after the 8-month test of 2020 indicate that the corrosivity of the test water was lower than in the first tests. In groundwater with nitrogen purging the corrosion rates were nearly constant, Figure 3. A small decrease in corrosion rates can be seen in the 2, 4, and 8-month tests in 2019. In the pore water test with air purging the corrosion rates showed the same decreasing trend as in air-purged groundwater in the 2019 and 2020 tests, Figure 4. There is a strong indication of passivation in the longer tests, even though this was not seen in all 8-month and 10-month tests. The corrosion rates in nitrogen-purged pore water were low, and they showed large

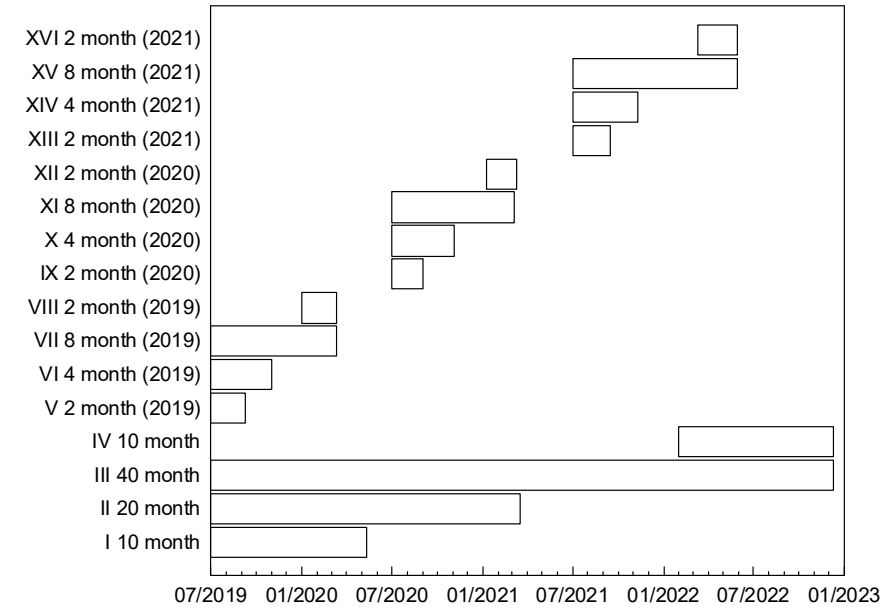

Figure 1. Timeline of long-term immersion tests.

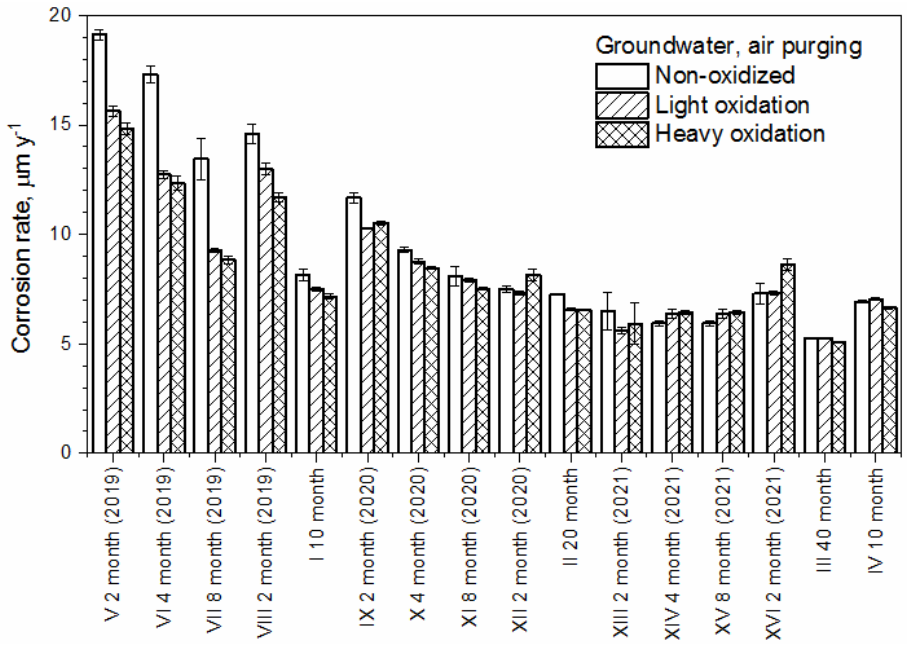

Figure 2. The corrosion rates in groundwater with air purging.

variations. The corrosion rates in nitrogen-purged waters did not show any clear decreasing trend with time.

The corrosion rates from long-term immersion tests are summarized in Table 2. The corrosion rates presented in Table 2 are averages of all the tests shown in Figures 2-5. The corrosion rates in Table 2 provided a baseline for corrosion rates at room temperature. In both waters, the initial corrosion rates are higher in air-purged waters than in

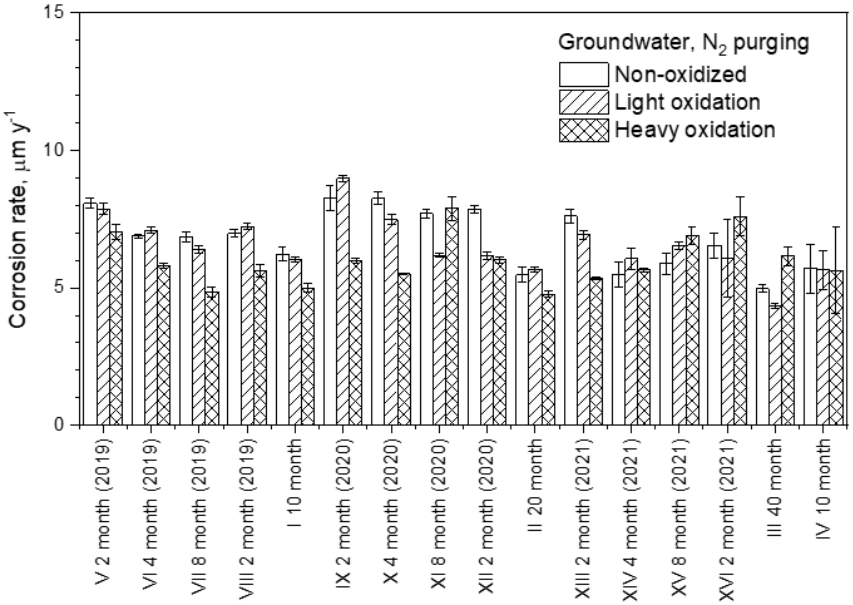

Figure 3. The corrosion rates in groundwater with nitrogen purging.

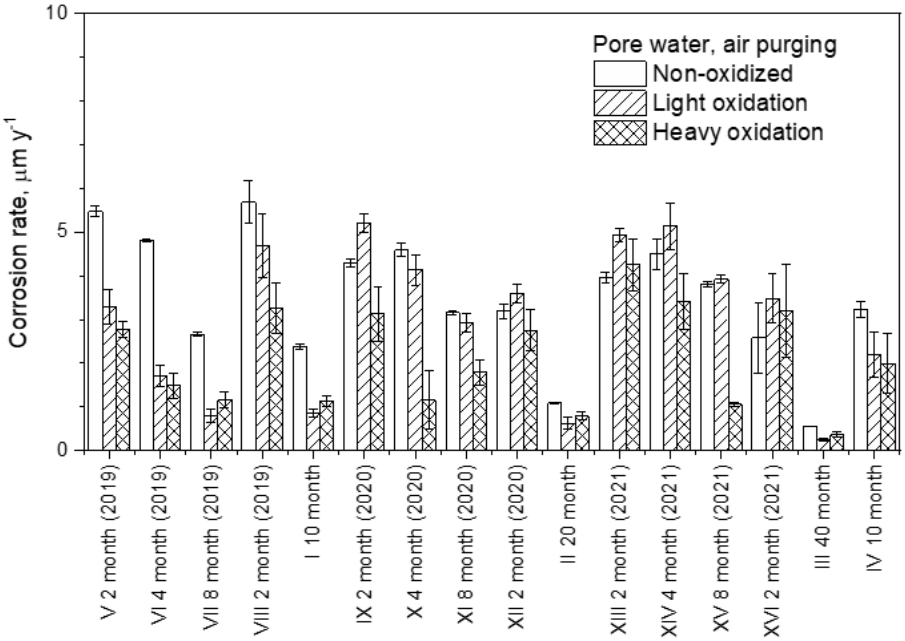

Figure 4. The corrosion rates in pore water with air purging.

nitrogen-purged waters. In groundwater, the corrosion rates decrease to the level of approximately 5 μm y^{-1} with time. In pore water, the corrosion rates decrease to less than one μm y^{-1} with time. The relative error was less than 5% except with oxidized samples in pore water, where it was 10 20%.

Short-term elevated temperature tests

Short-term elevated temperature tests were done at 40 °C, 60 °C and 80 °C. In the analysis, the 20 °C test corrosion rates are taken as averages of the six 2-month tests done at room temperature shown on the 1st row in Table 2. The corrosion rates increased

with temperature, but some of the pore water samples could not be properly cleaned because of the risk of excessive dissolution. The corrosion rates as a function of test temperature are shown in Figure 6.

To study the effect of temperature on the reaction mechanisms, activation energies were calculated using the Arrhenius equation (2), where CR is measured corrosion rate, A is the pre-exponential factor, E_A is the activation energy J mol^{-1}, R is the general gas constant 8.314 J mol^{-1} K^{-1} and T is absolute temperature in K. By determining the slope of ln(CR) vs. 1/T it is possible to calculate the activation energy by multiplying the slope value and error of the linear fit by the constant R. The slope and error were determined using Microsoft Excel Linest command.

$$CR = A \cdot \exp[-E_A/(R \cdot T)] \quad (2)$$

The calculated activation energies are shown in Table 3. The activation energies in groundwaters and in pore water with nitrogen purging indicate that the corrosion rate is determined by either a

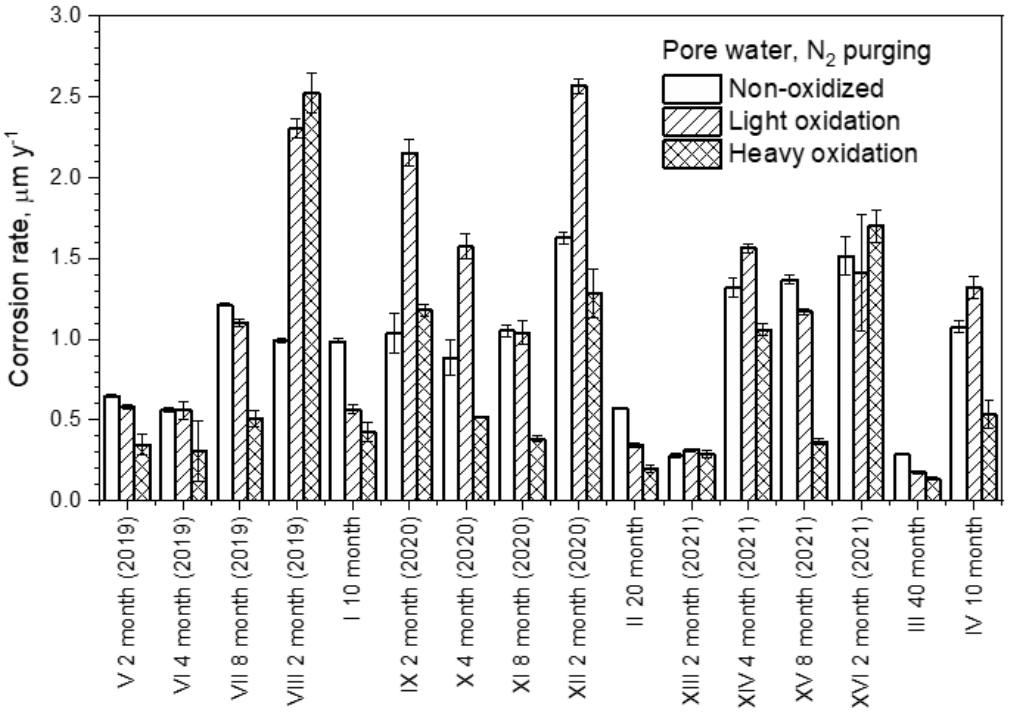

Figure 5. The corrosion rates in pore water with nitrogen purging.

Table 2. Average corrosion rates in µm y^{-1} from long-term immersion tests.

Test	Groundwater, air			Groundwater, N_2			Pore water, air			Pore water, N_2		
months	CU	LI	HE	CU	LI	HE	CU	LI	HE	CU	LI	HE
2	11.1	9.9	10.0	7.6	7.2	6.3	4.2	4.2	3.2	1.0	1.6	1.2
4	10.9	9.3	9.1	6.9	6.9	5.7	4.6	3.7	2.0	0.9	1.2	0.6
8	9.2	7.8	7.6	6.8	6.4	6.6	3.2	2.5	1.3	1.2	1.1	0.4
10	7.5	7.3	6.9	6.0	5.8	5.2	2.8	1.5	1.6	1.0	0.9	0.5
20	7.3	6.6	6.5	5.5	5.7	4.8	1.1	0.6	0.8	0.6	0.3	0.2
40	5.3	5.2	5.1	5.0	4.3	6.2	0.6	0.3	0.4	0.3	0.2	0.1

chemical or electrochemical process. The measured activation energies were lower than in various environments, where the reaction mechanism has previously been determined as chemical or electrochemical dissolution. For example, in 3% NaCl solution the activation energy has been measured as 39 kJ mol^{-1} [30]. In acid system with oxygen reduction as cathodic reaction the activation energy was 47 kJ mol^{-1} [31]. In alkaline solution the activation energy for oxidation of clean copper surface to Cu_2O was 81 kJ mol^{-1} [32]. The measured activation energies indicate that in the synthetic waters both charge transfer and mass transfer affect the corrosion rate. In pore water with air purging the activation energies were low, indicating that the rate-determining step is mass transfer. For example, in bicarbonate solutions with a porous reaction product layer, corrosion has been controlled by mass transfer with activation energy in the order of ~10 kJ mol^{-1} [33] and in natural sea water 15 kJ mol^{-1} [34]. In our tests, in every test environment the activation energies of oxidized and non-oxidized samples were the same. Therefore, it can be concluded that the air-formed oxide films did not affect the reaction mechanism.

Using the results shown in Figure 6 and Table 3, it was estimated that in groundwater with air purging the corrosion rate increases by a factor of 6-7 when temperature increases from 20 °C to 80 °C. In groundwater with nitrogen purging the corrosion rate increases by a factor of 3-4, in pore water with air purging by 2, and in pore water with nitrogen purging by 6-8.

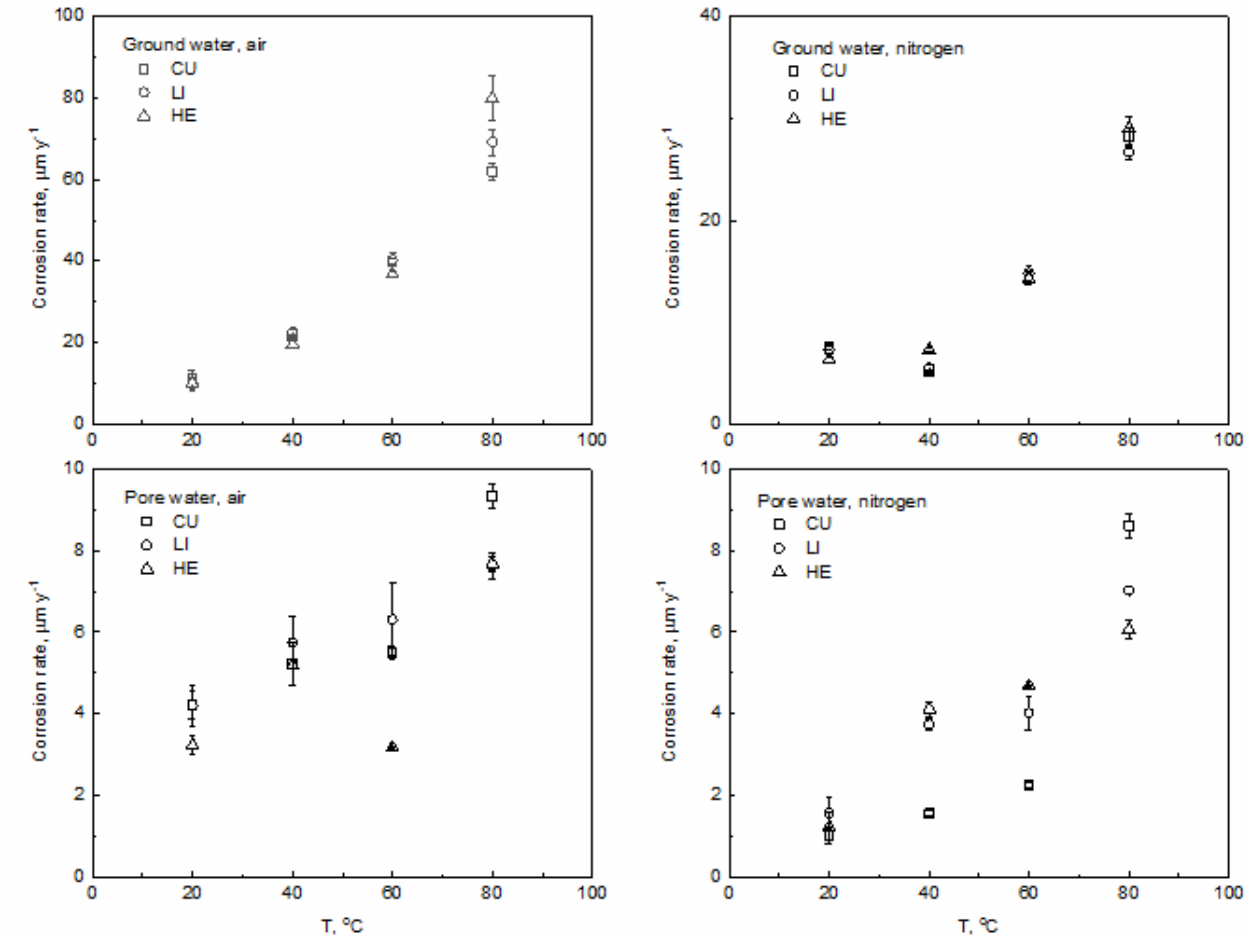

Figure 6. The effect of temperature on corrosion rates in all test environments.

Table 3. Activation energies of oxidized and non-oxidized samples.

Water	Gas	Oxidation	E_A (kJ mol^{-1})
GW	Air	None	26.0 ± 2.1
GW	Air	60°C, 3 days	27.8 ± 2.8
GW	Air	100°C, 7 days	28.5 ± 1.5
GW	N_2	None	15.4 ± 1.8
GW	N_2	60°C, 3 days	16.8 ± 1.8
GW	N_2	100°C, 7 days	19.8 ± 1.2
PW	Air	None	10.5 ± 2.6
PW	Air	60°C, 3 days	8.9 ± 1.7
PW	Air	100°C, 7 days	10.5 ± 2.7
PW	N_2	None	28.8 ± 3.6
PW	N_2	60°C, 3 days	25.7 ± 4.9
PW	N_2	100°C, 7 days	30.1 ± 4.9

The effect of oxide film on corrosion

The effect of the oxide film on corrosion was analyzed by comparing the corrosion rates between non-oxidized and oxidized samples in each test using the t-test: Two-Sample Assuming Unequal Variance. Examples of the t-test analysis and corresponding box-and-whisker chart are shown in Figure 7. Figure 7(a) shows the statistical analysis result when comparing the corrosion rates of the sample set CU GW-AIR with LI-GW-AIR and CU-GW-N2 with LI-GW-N2. If in the t-test the calculated two-tailed p-value, marked in Figure 7(a) as P(T<=t) two-tail, is smaller than the confidence level (α = 0.05) then there is a statistically significant difference in the mean values. In Figure 7(a), the comparison in air-purged water shows a difference, but the nitrogen-purged water does not. This is also shown in the box-and-whisker plot in Figure 7(b) as in the air-purged test the corrosion rate ranges do not overlap but in the nitrogen-purged test they do.

Figure 8 shows comparisons of corrosion rates between non-oxidized and oxidized samples. Every point in Figure 8 is an average of the five replicate samples from each of the 16 tests shown in the timeline Figure 1, and each of these tests included four environments. On the horizontal axis are the corrosion rates of non-oxidized samples and on the vertical axis are the oxidized samples from the same test. The pattern is clear, and the corrosion rates of neither lightly oxidized nor heavily oxidized samples differ much from the non-oxidized ones. The first analysis from Figure 8 is that the oxide films do not increase the corrosion rate significantly. Even though the corrosion rates varied between tests in the same environment (Figures 2 to 5), comparisons between oxidized and non-oxidized samples can be done. The tests in groundwater with air purging show that the oxide films gave some protection with short immersion times where corrosion rates were the highest. In air-purged groundwater, the corrosion rates of oxidized samples were lower than the non-oxidized ones, and these points are below the diagonal line. In groundwater with nitrogen purging, there is not as clear a difference. In pore water with air purging the oxide films seem to give some protection, whereas in pore water with nitrogen purging the oxide film can increase the corrosion rate.

To determine whether the differences in Figure 8 were significant, all tests were analyzed using the t-test as shown in Figure 7. A summary of the t-test analysis is shown in Figure 9. The comparisons using the t-test between oxidized and non-oxidized samples in the same test indicated that the oxide film produced by light oxidation protected in 23 cases, increased corrosion rate in 7 cases, and in 34 cases there was no difference. The oxide film produced by heavy oxidation

t-Test: Two-Sample Assuming Unequal Variances

	CU GW-AIR	*LI GW-AIR*
Mean	17.3369673	12.7329475
Variance	0.75955932	0.11801616
Observations	5	5
Hypothesized Mean Difference	0	
df	5	
t Stat	10.9895509	
P(T<=t) one-tail	5.4275E-05	
t Critical one-tail	2.01504837	
P(T<=t) two-tail	0.00010855	
t Critical two-tail	2.57058184	

	CU GW-N2	*LI GW-N2*
Mean	6.8899056	7.09683867
Variance	0.01681939	0.08043936
Observations	5	5
Hypothesized Mean Difference	0	
df	6	
t Stat	-1.4837153	
P(T<=t) one-tail	0.09420631	
t Critical one-tail	1.94318028	
P(T<=t) two-tail	0.18841262	
t Critical two-tail	2.44691185	

(a)

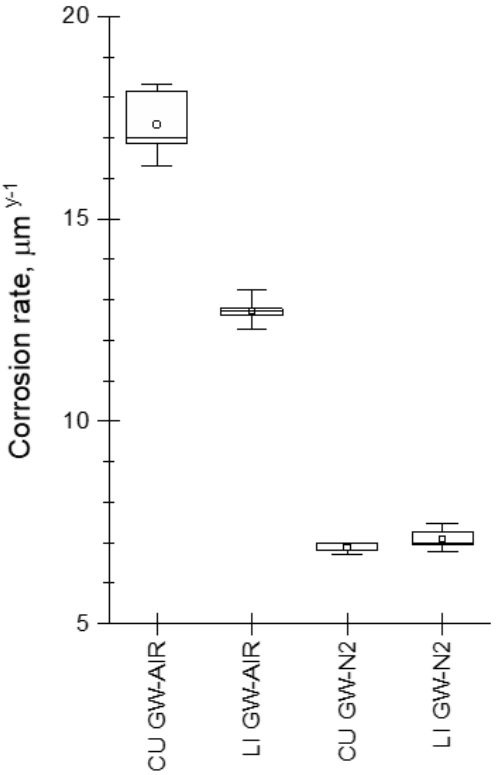

(b)

Figure 7. Statistical (a) and visual (b) analysis to determine, whether oxidized and non-oxidized samples have different corrosion rates.

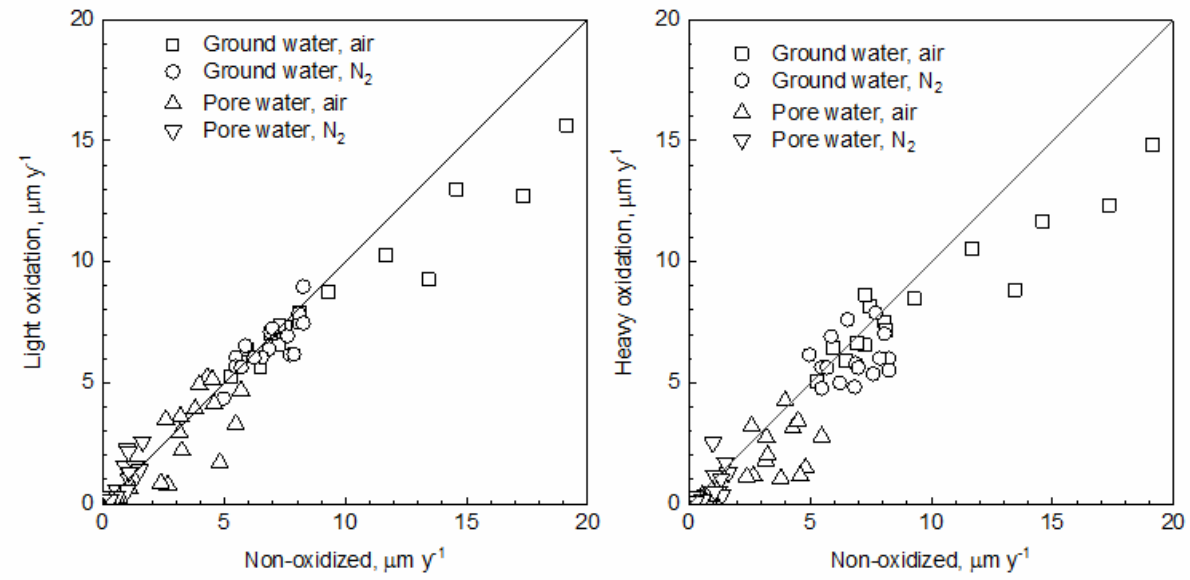

Figure 8. Corrosion rates of oxidized samples compared to non-oxidized samples in all test environments.

protected in 39 cases, increased corrosion rate in one, and in 24 cases there was no difference.

To determine the effect of oxide film at elevated temperatures the corrosion rates of non-oxidized and oxidized samples were compared by using t-test with unequal variances. The comparison results are shown in Table 4. In most of the test environments (19 out of 24), the oxide film did not affect the corrosion rate or gave protection. In some of the nitrogen-purged tests, the oxide film resulted in a higher corrosion rate.

The long-term corrosion tests provided a baseline, and as shown in Table 2, with immersion times of tens of months the corrosion rates in room temperature groundwaters decreased to 4 6 μm y^{-1} and in pore waters to less than one μm y^{-1}. The t-test results of the long-term tests (Figure 9) show that in 49% of the long-term tests the oxide films protected copper, in 45% there was no statistical difference, and in 6% the oxide film resulted in a higher corrosion rate. The short-term tests at elevated temperatures (Table 4) show that in 25% of the tests, the oxide film protected, in 54% there was no statistical difference and in 21% corrosion rate increased. To determine whether the oxide film can have a significant effect on the canister lifetime, it is necessary to study the absolute increases in the corrosion rate. In room temperature groundwater the oxide films did not increase the corrosion rate and in pore water, the maximum increase was 1.5 μm y^{-1} in 2-month tests. At elevated temperatures, the maximum increase in corrosion rate was 2.5 μm y^{-1}.

The nominal wall thickness of the KBS-3 copper canister is 50 mm. The maximum general corrosion allowance due to entrapped oxygen is 0.77 mm [6]. The increase of corrosion rate by a few μm y^{-1} during the first years will not significantly affect the canister's lifetime.

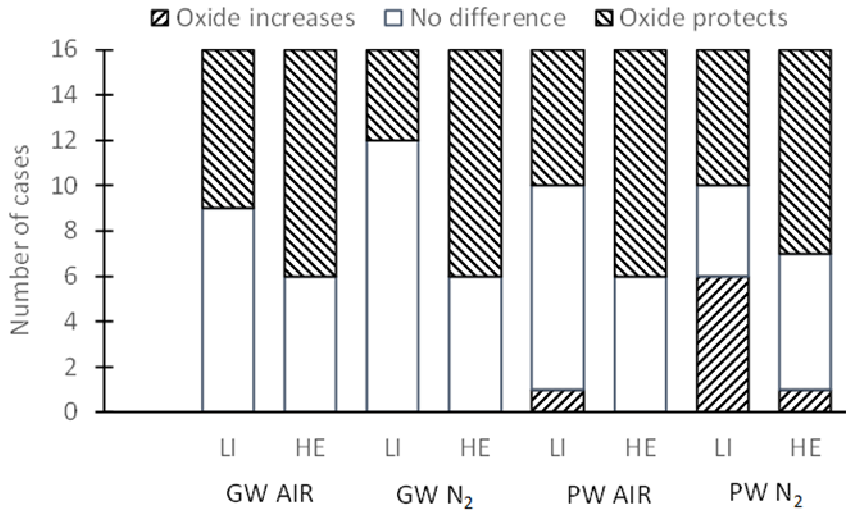

Figure 9. The results of t-test analysis to determine the significance of corrosion rate differences in the long-term tests.

Table 4. Comparison of oxidized and non-oxidized sample corrosion rates in different environments: + indicates protection by oxide film, o no statistically significant effect, and – increased corrosion rate by oxide film.

T, °C	GW air		GW N_2		PW air		PW N_2	
	LI	HE	LI	HE	LI	HE	LI	HE
40	o	o	o	-	o	o	-	-
60	o	+	o	o	o	+	-	-
80	o	o	o	o	+	+	+	+

Passivation

The passivation of copper depends on the pH of the environment. The concentration and speciation of dissolved copper depend on the nature of the solid copper compounds, pH, chloride concentration, and temperature. In alkaline solutions, the thermodynamically favored solids are Cu_2O and CuO. According to [35] there is a minimum solubility of copper at pH 9-12, and the minimum solubility is seen at higher pH when chloride concentration increases. At pH 8-8.5 the reaction product layer is $CuCl/Cu_2O/CuO$ that changes to $Cu_2O/CuO/Cu(OH)_2$ at pH 10-10.5. The $CuO/Cu(OH)_2$ is at least partly formed from the Cu_2O [35]. Passivation is more probable in a high pH and low chloride system. High sulfate, high carbonate, and low temperature promote passivation. Chloride concentration above 0.1 mol dm^{-3} (~3500 ppm) can prevent passivation [36].

Figure 10 shows copper samples after cleaning and after oxidation at 100 °C. There are no visible features on the clean copper surface and the analysis shows only Cu. The oxidized sample shows some darker islands that can be CuO. The Cu:O ratio, 91.5 at-% Cu, 8.3 at-% O, is higher than for the oxides Cu_2O and CuO. This is due to the thin oxide layers and the analysis also includes signals from the copper base material.

During the immersion tests, the copper samples developed different reaction product layers. Some examples of these are shown in Figure 11 with non-oxidized samples after 40 months of immersion at room temperature. SEM and XRD analyses showed that in groundwater with air purging the corrosion product layer consisted of 72-78% Cu, 19-22% O, 3-5% Cl, and less than 1% of S and Mg, and the identified compounds were Cu, Cu_2O and CuCl. In groundwater with nitrogen purging the product layer of non-oxidized and lightly oxidized samples consisted of 60% Cu, 25-28% O, 10-13% Cl and <1% S, and the compounds were Cu, Cu_2O and CuCl. The heavily oxidized samples had 90% Cu and 10% O, and only Cu and Cu_2O were identified. In air-purged pore water, the reaction product layers of non-oxidized samples consisted of 76% Cu and 24% O, and those of oxidized samples 61% Cu, 38% O and <1 % Mg. In nitrogen-purged pore water, the corrosion product layers consisted of 73-77% Cu and 23-27% O with small amounts of hardness salts Ca and Mg. The identified compounds were Cu, Cu_2O and $CuCO_3 \cdot Cu(OH)_2$. Some samples had excess oxygen when compared to copper oxides, so there were most likely copper sulfates and hydroxides even though they were not identified by XRD.

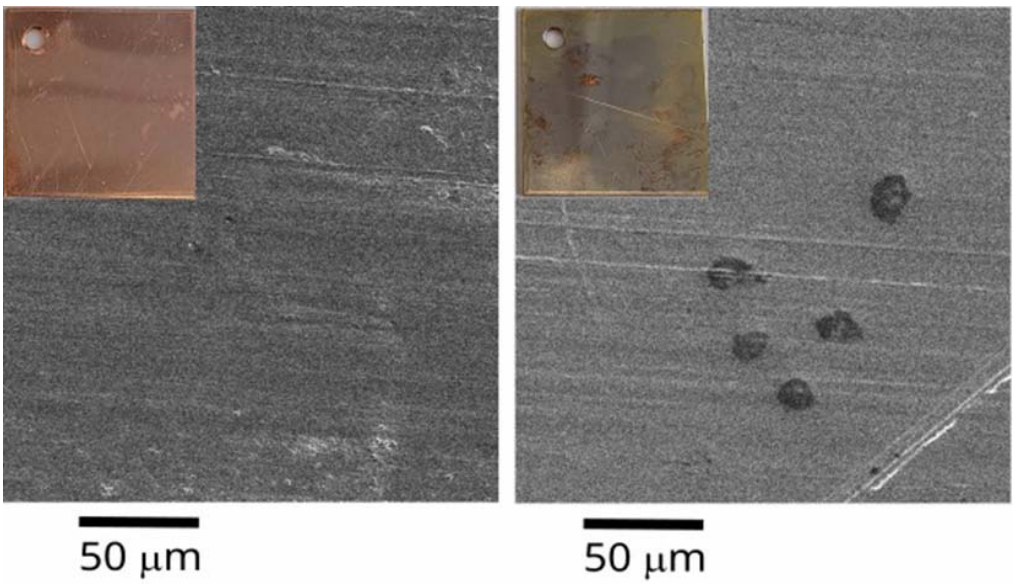

Figure 10. Surface features of cleaned and oxidized copper surfaces.

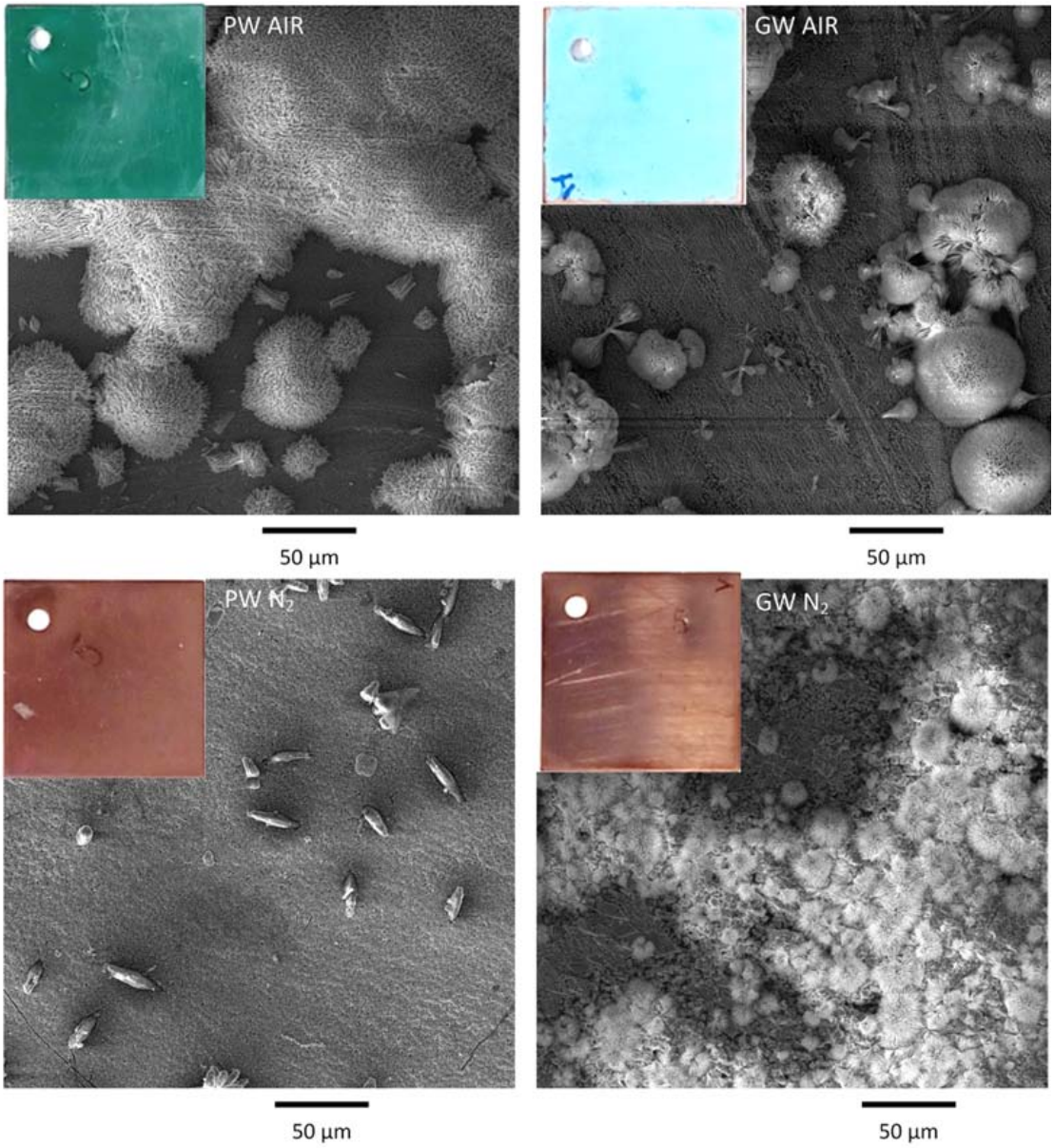

Figure 11. Corrosion product films after 40 months of immersion at room temperature.

DISCUSSION

The copper corrosion in neutral water with less than 1 M (35.45 g dm^{-3}) chlorides can follow different reaction mechanisms. The initial oxidation step can be reaction (3), or (4) & (5), or (6) & (7), where the mechanisms (3) and (4) & (5) represent the direct formation of a cuprous chloride species from the metal and (6) & (7) involve the dissolution of copper as a cuprous ion in the first instance [23].

$$Cu + 2\,Cl^- \rightarrow CuCl_2^- + e^- \quad (3)$$

$$Cu + Cl^- \rightarrow CuCl + e^- \quad (4)$$

$$CuCl + Cl^- \rightleftharpoons CuCl_2^- \quad (5)$$

$$Cu \rightarrow Cu^+ + e^- \quad (6)$$

$$Cu^+ + 2\,Cl^- \rightleftharpoons CuCl_2^- \quad (7)$$

The cuprous chloride complex can react to cuprous oxide by hydrolysis reaction (8) and increasing pH will favor the formation of the oxide [23]. The

cuprous chloride complex can also be oxidized to cupric ions (9) that could act as oxidants or most likely precipitate [7].

$$2\ CuCl_2^- + 2\ OH^- \rightarrow Cu_2O + H_2O + 4\ Cl^- \quad (8)$$

$$4\ CuCl_2^- + O_2 + 2\ H_2O \rightarrow 4\ Cu^{2+} + 8\ Cl^- + 4\ OH \quad (9)$$

The cathodic reaction is the reduction of oxygen (10) with intermediate hydrogen peroxide species. The hydrogen peroxide intermediates can oxidize cuprous ions to cupric [23].

$$O_2 + 2\ H_2O + 4\ e^- \rightarrow 4\ OH^- \quad (10)$$

Reduction of oxygen on cuprous oxide can result in the formation of cupric oxide by (11) & (12) and the cuprous oxide is regenerated by (13) [23].

$$Cu_2O + O_2 + H_2O \rightarrow 2\ CuO + H_2O_2 \quad (11)$$

$$Cu_2O + H_2O_2 \rightarrow 2\ CuO + H_2O \quad (12)$$

$$2\ CuO + H_2O + 2\ e^- \rightarrow Cu_2O + 2\ OH^- \quad (13)$$

The air-formed oxide film contains mainly Cu_2O. This oxide film can cover the metal surface fully and protect it from corrosion or it can have damages and promote cathodic reduction of oxygen and copper corrosion. The first reaction product of copper dissolution is $CuCl_2^-$ that can react to Cu_2O and further to CuO. CuO can be reduced back to Cu_2O. Cu_2O can react with chlorides, sulfates, and carbonates in the solution to form different corrosion products.

In the long-term tests at room temperature the oxide film produced by heavy oxidation (100 °C, 7 days) protected in 60% of the tests, and increased corrosion in one test (2%). The effect of the oxide film was not dependent on the test environment. In the short-term tests at elevated temperatures, the oxide films protected in 33% of the tests and increased corrosion rate in 25%. The corrosion rates increased in tests with nitrogen purging. The oxide film produced by light oxidation (60 °C, 3 days) protected in 36% of the long-term tests, and increased corrosion in 10%. In the short-term tests, the oxide films produced by light oxidation protected in 17% of the tests and increased corrosion rate also in 17% of the tests. The oxide film produced by light oxidation increased corrosion rates in tests with nitrogen purging.

The trends shown in Figure 9 and Table 4 indicate that the oxide films produced by the heavy oxidation are dense and protective. These oxide films can also contain CuO which inhibits oxygen reduction and decreases the rate of electrochemical corrosion reactions. The oxide films produced by light oxidation are thinner and not as dense as oxides produced by heavy oxidation. The presence of both metallic copper and Cu(I) species can increase the rate of oxygen reduction reaction causing an increase in corrosion rate.

The environmental variables in the tests were water composition, gas purging, and temperature. The most important variable in test water is pH. The higher pH of the pore water can result in the production of Cu_2O that can lead to more protective corrosion product film, reaction (8). In the long-term tests, the corrosion rates in air-purged pore water (pH = 10) were on average 25-40% of those in groundwater (pH = 8) and in nitrogen-purged pore water 12-18% of those in groundwater. The gas purging affects the concentration of dissolved oxygen. In the tests, the systems were either saturated with oxygen or oxygen-deficient, but with nitrogen-purging, it was not possible to get anoxic or reducing conditions. In nitrogen-purged groundwater, the corrosion rates were 70% of those in air-purged waters and in pore water 25-40%. An increase in temperature resulted in higher corrosion rates, but the reaction mechanism was not affected by the oxide films. Based on the activation energies, the corrosion in groundwater and in nitrogen-purged pore water was controlled by a chemical or electrochemical step. In pore water with air purging corrosion was controlled by a mass transfer step. The systems, where oxide film was seen to increase corrosion rate, were high pH and nitrogen-purging. These systems should show the lowest corrosion rates, see Figure 8. It is possible that the oxide films could promote oxygen reduction so that a change in corrosion rate was seen even though the actual corrosion rates are very low.

The copper canisters for the spent nuclear fuel should last intact for hundreds of thousands of years. Information about the corrosion rates is available only from tests with maximum test times of years. The topic of this study was to determine whether an oxide film can result in a higher

corrosion rate during the first years of emplacement and if the oxide film can significantly affect the lifetime of the canister. The nominal wall thickness of the copper canister in the KBS-3 concept is 50 mm. In the safety cases analysis, the maximum general corrosion allowance due to entrapped oxygen is 0.77 mm [6]. The long-term corrosion tests showed that with immersion times of tens of months, the corrosion rates in room temperature groundwaters decreased from initial 15-20 μm y^{-1} to 4 6 μm y^{-1} and in pore waters from initial 5 μm y^{-1} to less than one μm y^{-1}. In room temperature groundwater the oxide films did not increase the corrosion rate and in pore water, the maximum increase was 1.5 μm y^{-1} in 2-month tests. At elevated temperatures, the maximum increase in corrosion rate was 2.5 μm y^{-1}. The warm and oxidizing period at the beginning of the final disposal will last only few years at maximum. Therefore, we can conclude that the small increases of corrosion rate by few μm y^{-1} during the first years will not significantly decrease the canister lifetime.

CONCLUSIONS

The corrosion rate of oxygen-free copper in synthetic groundwater at room temperature decreased from an average 6-11 μm y^{-1} in 2-month tests to 4-6 μm y^{-1} in 40-month tests. In synthetic pore waters at room temperature, the corrosion rates were on average 1-4 μm y^{-1} in 2-month tests decreasing to less than one μm y^{-1} in 40-month tests.

An increase in temperature from 20 °C to 80 °C resulted in maximum corrosion rates of 60-80 μm y^{-1} in air-purged groundwater and 30 μm y^{-1} in nitrogen-purged groundwater. In air-purged pore water, the highest corrosion rates were 8-9 μm y^{-1} and in nitrogen-purged pore water 2-4 μm y^{-1}, both at 80 °C.

The effect of the air-formed oxide film was evaluated by comparing the corrosion rates of oxidized and non-oxidized samples. In most of the tests, the oxide films protected slightly or had no effect. The oxide film increased corrosion in some tests with nitrogen-purged pore water. This was usually seen with the samples treated with light oxidation. However, as the corrosion rate changes were only a few μm y^{-1}, it was concluded that the oxide films do not affect the canister operational time.

ACKNOWLEDGEMENTS

This research was funded by The Ministry of Economic Affairs and Employment financed project OXCOR (The effect of oxide layer on copper corrosion in repository conditions) in the Finnish Research Programme on Nuclear Waste Management (KYT2022). This study utilized the Academy of Finland's RawMatTERS Finland Infrastructure (RAMI) based jointly at Aalto University, GTK, and VTT in Espoo.

CONFLICT OF INTEREST STATEMENT

The authors declare no conflict of interest. The funders had no role in the design of the study; in the collection, analyses, or interpretation of data; in the writing of the manuscript, or in the decision to publish the results.

REFERENCES

1. Storage and Disposal of Radioactive Waste. Available online: https://world-nuclear.org/information-library/nuclear-fuel-cycle/nuclear-waste/storage-and-disposal-of-radioactive-waste.aspx (accessed on 8.8.2023).
2. Svensk Kärnbränslehantering AB 2010, Utvecklingen av KBS-3-metoden Report SKB R-10-40, Svensk Kärnbränslehantering AB, Stockholm, 293.
3. Posiva Oy 2017, Safety Case Plan for the Operating Licence Application Report POSIVA 2017-02, Posiva Oy, Eurajoki, 152.
4. Posiva Oy, Svensk Kärnbränslehantering AB 2017, Safety functions, performance targets and technical design requirements for a KBS-3V repository, Posiva SKB Report 01, Posiva & SKB: Eurajoki, 116.
5. King, F. and Kolář, M. 2019, Corrosion, 75, 309.
6. Posiva Oy 2021, Canister Evolution Working Report 2021-06 Posiva Oy, Eurajoki, 342.
7. King, F., Kolář, M. and Maak, P. 2008, J. Nuc. Mat., 379, 133.
8. King, F., Lilja, C. and Vähänen, M. 2013, J. Nuc. Mat., 438, 228.
9. Huttunen-Saarivirta, E., Rajala, P., Bomberg, M. and Carpén, L. 2017, Appl. Surf. Sci., 396, 1057.
10. Saario, T., Mäkelä, K., Laitinen, T. and Bojinov, M. Susceptibility of copper to general

and pitting corrosion in saline groundwater; Report STUK-YTO-TR 176, Radiation and Nuclear Safety Authority, Helsinki, 18.
11. Laitinen, T., Mäkelä, K., Saario, T. and Bojinov, M. 2001, Susceptibility of copper to general and pitting corrosion in highly saline groundwater SKI Report 01:2, Swedish Nuclear Power Inspectorate, Stockholm, 24.
12. Rosborg, B., Kranjc, A., Kuhar, V. and Legat, A. 2011, Corros. Eng. Sci. Technol., 46, 152.
13. Wersin, P. 2013, LOT A2 test parcel, Compilation of copper data in the LOT A2 test parcel SKB Technical Report TR-13-17, Swedish Nuclear Fuel and Waste Management, Stockholm, 28.
14. Tully, C. S., Binns, W. J., Zagidulin, D. and Noël, J. J. 2023, Mater. Corros, 74, 1677.
15. Johansson, A. J., Lilja, C. and Hedin, A. 2019, Proceedings of the IHLRWM 2019, Knoxville, Tennessee, 316.
16. Karnland, O., Sandén, K., Johannesson, L.-E., Eriksen, T. E., Jansson, M., Wold, S., Pedersen, K., Motamedi, M. and Rosborg, B. 2000, Long term test of buffer material SKB Technical Report TR-00-22, Swedish Nuclear Fuel and Waste Management, Stockholm, 131.
17. Kinnunen, P., Saario, T. and Betova, I. 2003, Evaluation of sensors to monitor the effect of bentonite on the corrosion rate of copper in Olkiluoto-type saline groundwater Report STUK-YTO-TR 197, Radiation and Nuclear Safety Authority, 20.
18. Raiko, H., Pastina, B., Jalonen, T., Nolvi, L., Pitkänen, J. and Salonen, T. 2012, Canister Production Line 2012 Report POSIVA 2012-16, Posiva Oy, Eurajoki, 174.
19. King, F., Lilja, C., Pedersen, K., Pitkänen, P. and Vähänen, M. 2012, An Update of the State-of-the-art Report on the Corrosion of Copper Under Expected Conditions in a Deep Geologic Repository Report POSIVA 2011-01, Posiva Oy, Eurajoki, 246.
20. Nolvi, L. 2009, Manufacture of Disposal Canisters Report POSIVA 2009-03, Posiva Oy, Eurajoki, 76.
21. Aromaa, J., Kekkonen, M., Mousapour, M., Jokilaakso, A. and Lundström, M. 2021, CMD, 2, 625.
22. Vazquez, M. V., de Sanchez, S. R., Calvo, E. J. and Schiffrin, D. J. 1994, J Electroanal. Chem., 374, 189.
23. Kear, G., Barker, B. D. and Walsh, F. C. 2004, Corros. Sci., 46, 109.
24. King, F., Quinn, M. J. and Litke, C. D. 1995, J. Electroanal. Chem., 385, 45.
25. Vukmirovic, M. B., Vasiljevic, N., Dimitrov, N. and Sieradzki, K. 2003, J. Elchem. Soc., 150, B10.
26. Benzbiria, N., Zertoubi, M. and Azzi, M. 2020, SN Appl. Sci., 2, 1.
27. Benzbiria, N., Zertoubi, M. and Azzi, M. 2021, Appl. Surf. Sci. Adv., 4, 1.
28. Huttunen-Saarivirta, E., Rajala, P. and Carpén, L. I. 2016, El. Acta, 203, 350.
29. Vikman, M., Matusewicz, M., Sohlberg, E., Miettinen, H., Järvinen, J., Itälä, A., Rajala, P., Raulio, M., Itävaara, M., Muurinen, A., Tiljander, M and Olin, M. 2018, Long-term experiment with compacted bentonite VTT Technology Report No. 332, VTT Technical Research Centre of Finland, Espoo, 84.
30. Otmacic, H. and Stupnisek-Lisac, E. 2003, El. Acta, 48, 985.
31. Lu, B. C. and Graydon, W. F. 1954, Can. J. Chem., 32, 153.
32. Dignam, M. J. and Dibbs, D. B. 1969, Can. J. C., 48, 1242.
33. Drogowska, M., Brossard, L. and Ménard, H. 1993, J. Elchem. Soc., 140, 1247.
34. Deyab, M. A., Essehli, R. and El Bali, B. 2015, RSC Advances, 5, 64326.
35. King, F. 2002, Corrosion of copper in alkaline chloride environments Technical Report TR-02-25, SKB: Stockholm, 77.
36. Qin, Z., Daljeet, R., Ai, M., Farhangi, N., Noël, J. J., Ramamurthy, S., Shoesmith, D., King, F. and Keech, P. 2017, Corros. Eng. Sci. Technol., 52, 45.